

# Surface adsorption of model dendrimers

Marc L. Mansfield

Michigan Molecular Institute, 1910 West St. Andrews Road, Midland, MI 48640, USA  
 (Received 3 October 1995)

Lattice model dendrimers interacting with an adsorbing planar surface are studied by computer simulation, where  $G$  is the number of generations of the dendrimer and  $A$  is the interaction strength. With increasing  $A$ , dendrimers are observed to spread out and flatten down on the surface, as expected. In certain regions of  $G$ - $A$  space, two competing configurational states,  $S_2$  and  $S_3$ , are observed. In  $S_3$  all three dendrons are adsorbed on the plane. In  $S_2$  two dendrons are adsorbed, while the third sits up and away from the surface.  $G$ - $A$  space divides into five separate regions: a desorption region where  $A$  is too weak to maintain adsorption, a weak adsorption region in which the dendrimer tends to maintain contact but with only weak perturbation of its shape, a region in which  $S_2$  and  $S_3$  compete because they have comparable free energies and are separated by a modest free energy barrier, a region in which  $S_3$  dominates because it has lower free energy, and finally a region in which  $S_2$  and  $S_3$  both have high stabilities because they are separated by a large free energy barrier. Copyright © 1996 Elsevier Science Ltd.

(Keywords: dendrimers; adsorption; Monte Carlo calculations)

## INTRODUCTION

Dendrimers are macromolecules with tree-like architectures. Previous publications report a number of properties of model dendrimers studied by computer simulation<sup>1-7</sup>. This paper reports results for computer-modelled lattice dendrimers adsorbed on surfaces. Adsorption of linear macromolecules has been studied extensively, but no theoretical work or computer studies have been reported for dendrimer adsorption. The problem is relevant to a number of possible applications of dendrimers that involve interaction with or adsorption onto surfaces<sup>8</sup>.

The model dendrimers are constructed on the diamond lattice, with structures shown schematically in *Figure 1*. *Figure 1* also displays our convention for defining the generation number,  $G$ , of a dendrimer. The simulation techniques employed in this study, including the Monte Carlo procedure, are nearly the same as those described in ref. 5.

## COMPUTATIONAL DETAILS

The diamond lattice may be generated in the following way. First define the following eight vectors:

$$\begin{aligned}
 \mathbf{a} &= (1, 1, 1) \\
 \mathbf{b} &= (-1, -1, 1) \\
 \mathbf{c} &= (-1, 1, -1) \\
 \mathbf{d} &= (1, -1, -1) \\
 \mathbf{a}' &= -\mathbf{a} \\
 \mathbf{b}' &= -\mathbf{b} \\
 \mathbf{c}' &= -\mathbf{c} \\
 \mathbf{d}' &= -\mathbf{d}
 \end{aligned}
 \tag{1}$$

Length units are such that each of these vectors has length  $\sqrt{3}$ . The lattice consists of the origin plus all points that can be written as a sum of a sequence of the above eight vectors provided that the first vector in the sequence is unprimed and that all subsequent vectors in the sequence alternate between being primed and unprimed. So, for example,  $\mathbf{a} + \mathbf{b} + \mathbf{a}$  is not on the lattice, but  $\mathbf{a} + \mathbf{b}' + \mathbf{a}$  is. In any one step, all three coordinates increase or decrease by one unit. Therefore, all three coordinates alternate from odd to even parity as we step through the lattice, and therefore, each lattice site exists in a well defined parity class.

Equivalently, we can generate the lattice from a cubic unit cell, with side of length 4 and containing eight lattice sites. The lattice consists of all those points  $4(i, j, k) + \mathbf{v}_m$ , where  $i, j$  and  $k$  are any integers, and where  $\mathbf{v}_m$  represents any one of the following eight vectors:

$$\begin{aligned}
 \mathbf{v}_0 &= (0, 0, 0) \\
 \mathbf{v}_1 &= (2, 2, 0) \\
 \mathbf{v}_2 &= (1, 1, 1) \\
 \mathbf{v}_3 &= (3, 3, 1) \\
 \mathbf{v}_4 &= (0, 2, 2) \\
 \mathbf{v}_5 &= (2, 0, 2) \\
 \mathbf{v}_6 &= (1, 3, 3) \\
 \mathbf{v}_7 &= (3, 1, 3)
 \end{aligned}
 \tag{2}$$

The dendrimer is confined in a cubical box of size 180 (45 unit cells on a side). It adsorbs on the basal plane ( $z = 0$ ) of the cube through an interaction to be described shortly. The core of the dendrimer is restricted to lie on sites of even parity within a column of unit cells running up the length of the box, i.e. any of the points

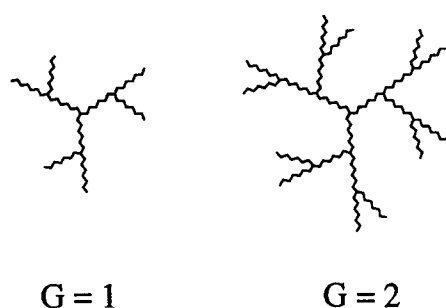


**Figure 1** Dendrimers are modelled on the diamond lattice. Each spacer includes seven lattice steps. The core and each branch point are trifunctional. To model adsorption, all the termini and certain branch points interact with a certain lattice plane, while all segments of the molecule are constrained to lie above that same plane

$4(0, 0, k) + \mathbf{v}_m$  where  $k$  is a non-negative integer and  $m = 0, 1, 4, \text{ or } 5$ . With this restriction the dendrimer is never able to interact with the lateral faces of the box, and it can only interact with the upper face by desorbing. Therefore, there is no need to impose periodic boundaries.

Each spacer of the dendrimer consists of seven lattice steps. This implies that the two ends of any one spacer have opposite parity. Since the core is always on a site of even parity, then the first tier of branch points all have odd parity, the second tier all have even parity, etc. The terminal segments all have parity opposite that of the quantity  $G$ .

All segments of the molecule are excluded from the zone  $z < 0$ . This automatically restricts all branch points and the molecular core from the plane  $z = 0$ . Any lattice site  $(x, y, z)$  is connected to four others on the lattice, two of which lie at  $z - 1$  and two at  $z + 1$ . Each branch point is, by definition, connected to three of these four sites, so any branch point  $z$  is connected to at least one site at  $z - 1$ . Therefore, branch points of even parity can come no closer to the forbidden region than  $z = 2$ . Branch points of odd parity can come as close as  $z = 1$ . All other segments of the molecule can reach either  $z = 0$  or  $z = 1$ , depending on their parity.

In addition to this hard-core repulsion, the molecule is attracted to the basal plane of the box as follows. Any branch points of the first, third, fifth, etc. tiers (i.e. any branch points of odd parity) found at  $z = 1$  contribute  $-AkT$  to the total energy. Any terminal segment found at either  $z = 0$  or  $z = 1$  also contributes  $-AkT$  to the total energy. All other segments contribute nothing. In this way,  $A$  becomes a measure of the strength of the adsorption interaction.

(There is no particularly good reason to assume that only odd branch points attach to the plane. In fact, the algorithm was specifically designed so that even branch points would attach at  $z = 0$ , and it was only rather near the completion of the project that it was realized that  $z = 0$  was inaccessible to these points. In spite of this rather peculiar interaction, the model is relevant. It still possesses many interesting properties that can be expected of real dendrimers adsorbing onto a planar surface.)

In previous computations on isolated dendrimers, it was obviously not necessary to move the central core of the molecule. However, we must now permit the relative distance between the core and the adsorption boundary

to fluctuate. This is done by performing, along with the internal wiggles and end wiggles described previously<sup>5</sup>, what we call 'core wiggles'. These are identical to internal wiggles but are performed in such a way as to permit the core to move. For example, Figure 2 of ref. 5 can be thought of as a diagram of a core wiggle if the moving branch point is assumed to be the molecular core.

To perform a wiggle, first an integer  $m$  between 0 and  $N$  inclusive, where  $N$  is the total number of spacers, is chosen at random. If  $m = 0$ , a core wiggle is attempted. Otherwise, attention is focused on the  $m$ th spacer. If the  $m$ th spacer is a terminal spacer, then an end wiggle is attempted on that spacer, and if it is not, then an internal wiggle is attempted on that spacer and its two daughter spacers. Metropolis biasing is employed to bring the system to thermal equilibrium. All other details concerning the wiggles are described in ref. 5.

The initial state of the dendrimer in any given run is obtained in any of a number of different ways. As described in ref. 5, we tolerate segment overlap at the outset of a run; this permits a rather wide range of techniques for initiating the run. All the following techniques were employed: (1) initiate the dendrimer as an all-*trans* linear chain lying near the basal plane, with complete overlap of all segments a given chemical distance from the core. Obviously, this produced copious overlaps at the outset but these disappear rather quickly, especially in the lower generations. Segments explode out from this initial configuration, some of these impinge on the basal plane, and at sufficiently large  $A$  the molecule evolves into a state of equilibrium adsorption. (2) Use a structure with the same number of generations but previously equilibrated at a different value of  $A$ . (3) Add a generation to a previously equilibrated structure of  $G-1$  generations simply by adding a pair of seven-step random walks to each terminus, with the only constraint that these walks cannot enter the region  $z < 0$ . These structures are generally also overlapped, but again, all the overlaps eventually disappear.

A sequence of wiggles is performed to bring the sample to equilibrium. The structures were deemed to have equilibrated when all overlaps had disappeared, and when other properties, such as the parallel and perpendicular components of the radius of gyration and the number of adsorbed segments, had stabilized. Anywhere from about four to 10 independent runs were performed at each value of  $G$  and  $A$ . The relaxation time is obviously a strong function of  $G$ , and so the sampling runs at higher  $G$  were typically much longer. Table 1 reports the average sample size as a function of  $G$ . As is

**Table 1** Sample size as a function of  $G$ , approximate number of attempted wiggles at each value of  $A$  and  $G$ , in units of  $10^9$  wiggles

$G$	$10^9$ wiggles
1	0.11
2	0.15
3	0.14
4	0.62
5	1.43
6	2.85
7	2.47
8	8.53

Each entry counts wiggles from at least a few independent runs but does not count wiggles performed to equilibrate the system

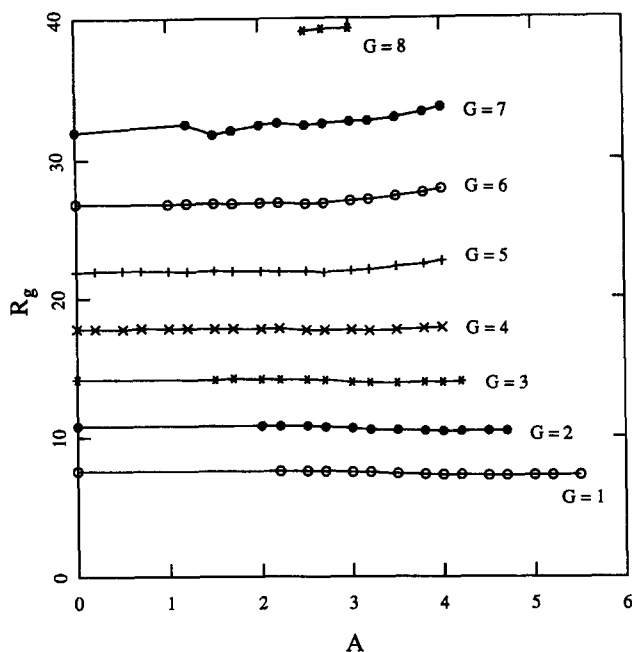


Figure 2 Radius of gyration as a function of  $A$  and  $G$

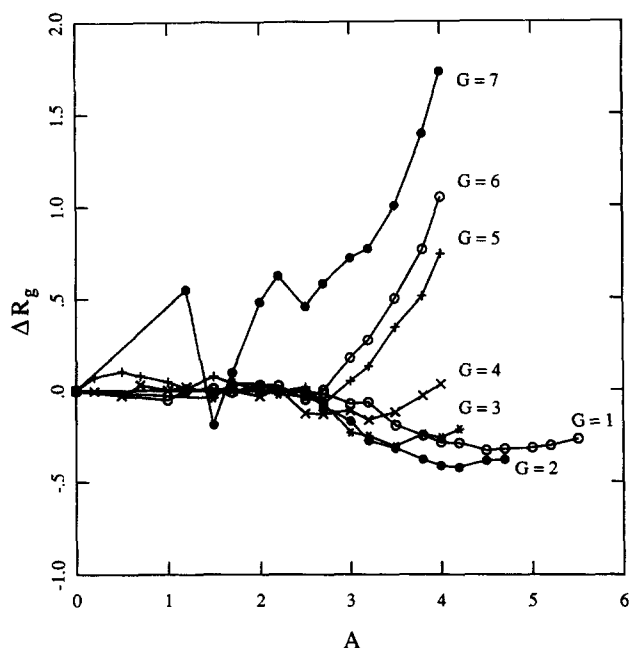


Figure 3 Change in radius of gyration relative to the unadsorbed ( $A = 0$ ) dendrimer

obvious from Table 1, considerable effort was exerted at  $G = 8$ , but with only mixed results, because of the long relaxation times of these large dendrimers. For example, it proved unfeasible to study a wide range of  $A$  values at  $G = 8$ . However, at all lower values of  $G$ , it was possible to study the system between the two extremes of weak and strong adsorption.

## RESULTS

Figure 2 displays radius of gyration data for the adsorbed dendrimers. The  $R_g$  values at  $A = 0$  are in good agreement with the data<sup>5</sup> already obtained for

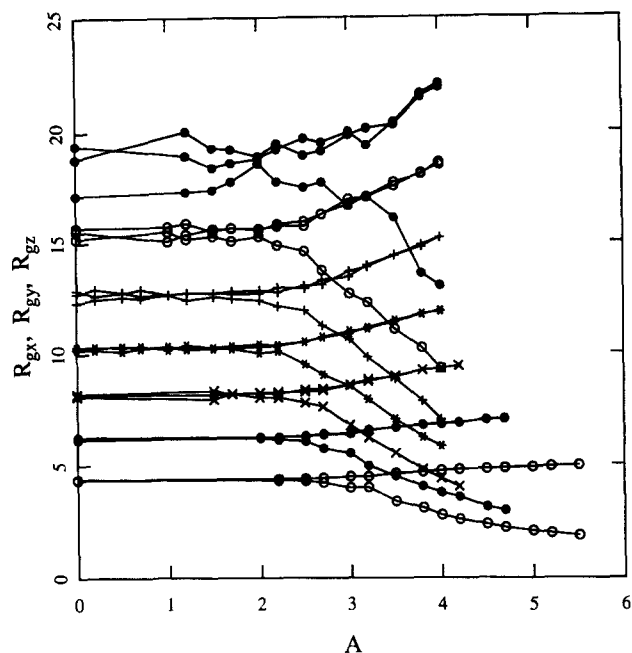


Figure 4  $R_{gx}$  and  $R_{gy}$  are components of  $R_g$  parallel to the adsorption plane,  $R_{gz}$  is the perpendicular component.  $R_{gx}$  and  $R_{gy}$  both increase with  $A$ , while  $R_{gz}$  decreases

isolated dendrimers, as expected. Interestingly, the overall radius of gyration is practically insensitive to the strength of the attraction, although as demonstrated in Figure 3,  $R_g$  shows a weak downward trend in the lower generations and a somewhat stronger upward trend in the higher generations. Nevertheless, the parallel and perpendicular components of the radius of gyration change more dramatically as  $A$  increases, as shown in Figure 4. Again, these trends are to be expected, the dendrimers are obviously flattening down and spreading out on the surface as  $A$  increases. These opposing trends in the parallel and perpendicular components tend to compensate, which explains the relative intensity of  $R_g$  to  $A$ .

Figure 5 displays the average  $z$  coordinate of the core, or in other words the average height of the core above the basal plane. The trends observed in Figure 5 are to be expected, and provide further quantification of the degree to which the dendrimer flattens out as  $A$  increases.

As described above, every terminal segment of the molecule as well as every branch point in the first, third, fifth, etc. tiers of branches stick to the basal plane whenever they make contact. Figure 6 displays the average number of such segments in contact with the plane as a function of  $A$ . For example, there are on average anywhere from between about two to about eight segments attached for  $G = 1$  dendrimers in the range of  $A$  values displayed, and from about four to about 200 for  $G = 7$ . This is significant because at  $G = 1$ , any of nine segments would attach to the plane if they made contact, while at  $G = 7$ , any of 639 segments are able to stick. Therefore, at low  $G$  and large  $A$  the dendrimer is sufficiently deformable that almost all segments available for attachment actually come into contact. On the other hand, at large  $G$ , the molecule is much less deformable, and only a relatively small fraction of the total is able, at any given time, to be in contact.

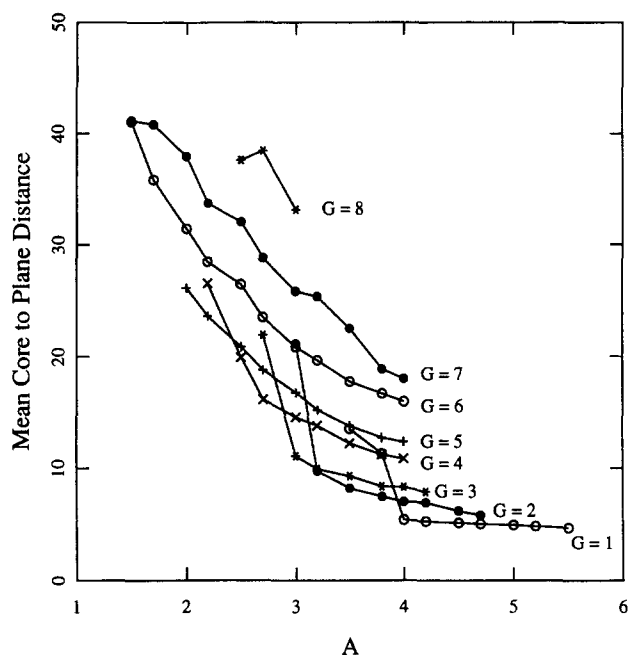


Figure 5 Mean distance of the molecular core above the basal plane

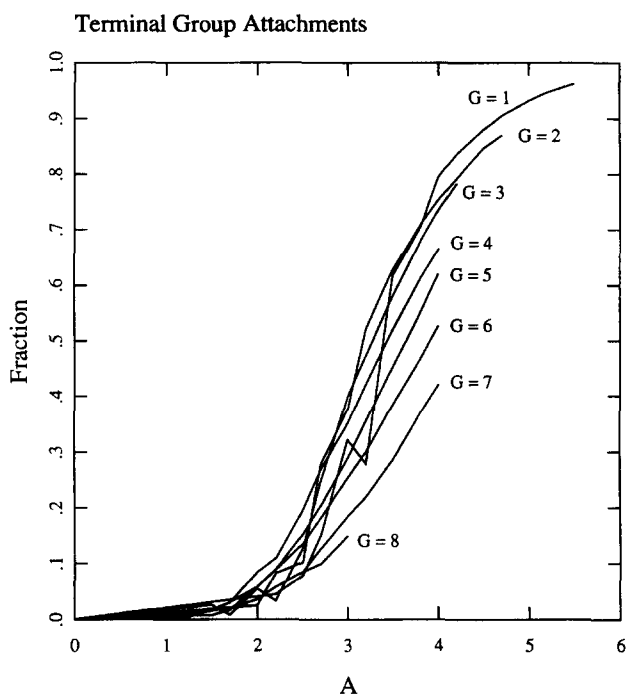


Figure 7 The average fraction of terminal groups that are found interacting with the basal plane

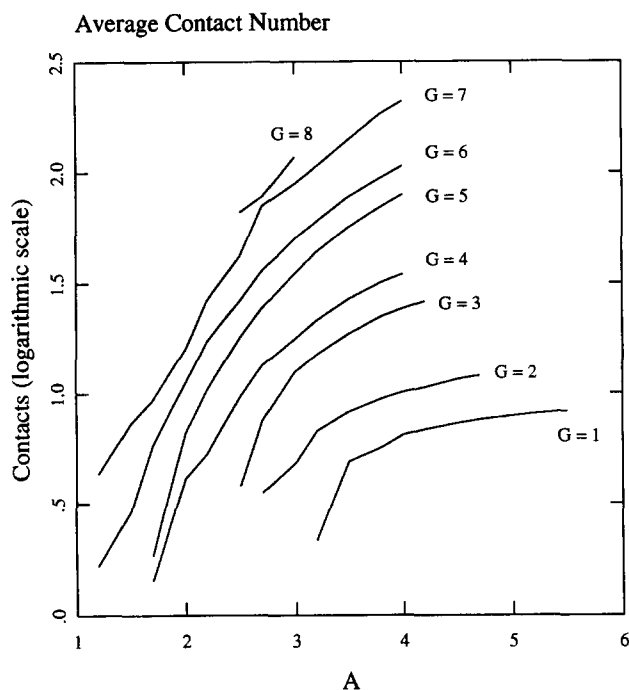


Figure 6 Decimal logarithm of the average number of contacts between the dendrimer and the adsorption surface

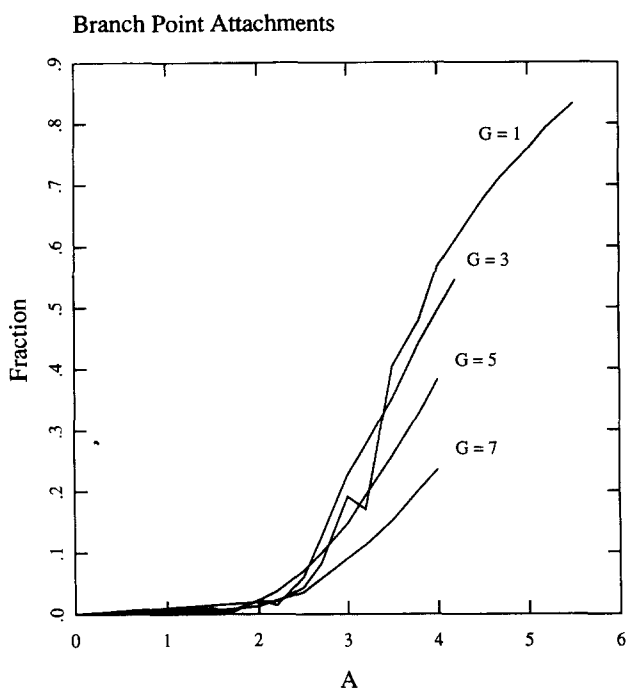
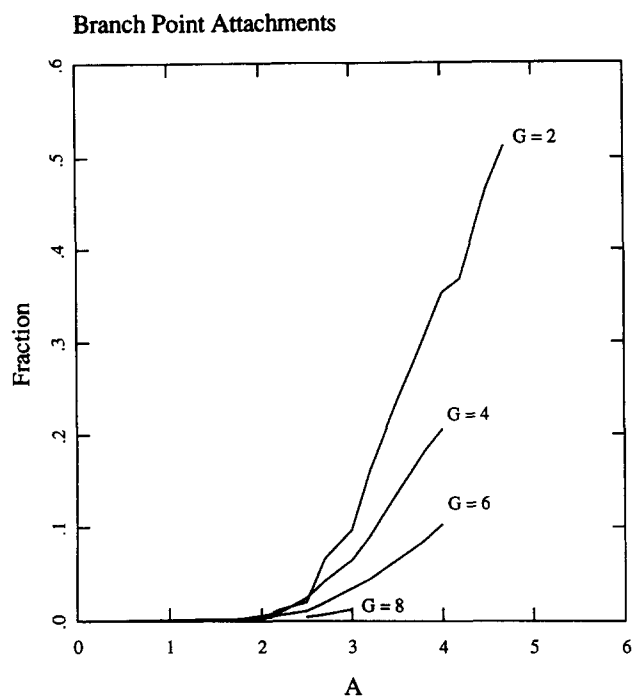


Figure 8 The average fraction of branch points exactly one spacer away from the termini found interacting with the basal plane. As explained in the text, such interactions only exist for dendrimers of odd  $G$

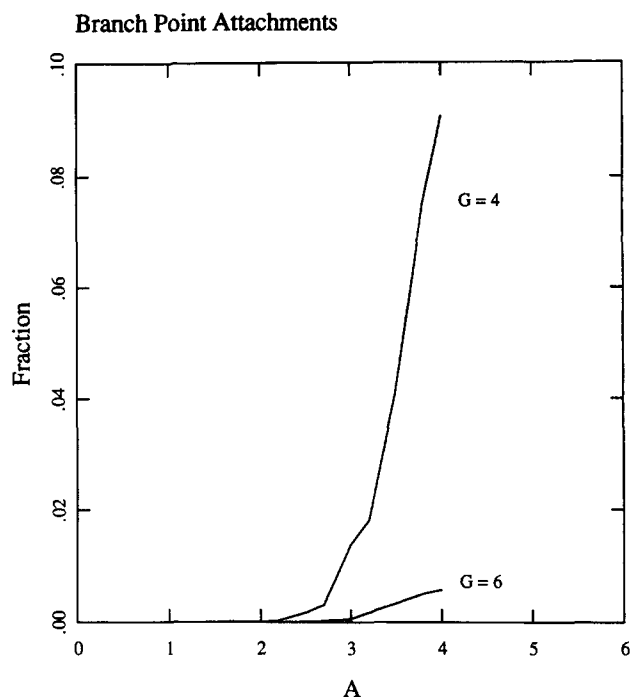
Of course the number of segments in contact increases as  $A$  increases, but it is also interesting to examine which segments the dendrimer chooses to place in contact with the plane. Figure 7 displays the fraction of terminal groups that are found in contact with the basal plane at given values of  $A$  and  $G$ . Likewise, Figure 8 displays the analogous fraction for the outer tier of branch points, as do Figures 9–11, but in progressively deeper tiers of branch points. Obviously, at any given values of  $G$  and  $A$  the dendrimer makes most of its contacts with the basal plane through the terminal groups, and fewer and fewer contacts are formed as we proceed to groups closer to the core.

Figure 12 displays a ‘phase’ diagram in  $G$ – $A$  space which is divided into five separate regions. Each region of the diagram corresponds to different behaviour of the dendrimer.

The desorption region of the phase diagram is characterized by small values of  $A$ . Any flexible macromolecule must give up configurational entropy to sit close to a barrier. If the adsorption energy is too small



**Figure 9** The average fraction of branch points exactly two spacers away from the termini found interacting with the basal plane. Only dendrimers of even  $G$  exhibit such interactions



**Figure 11** The average fraction of branch points exactly four spacers away from the termini found interacting with the basal plane

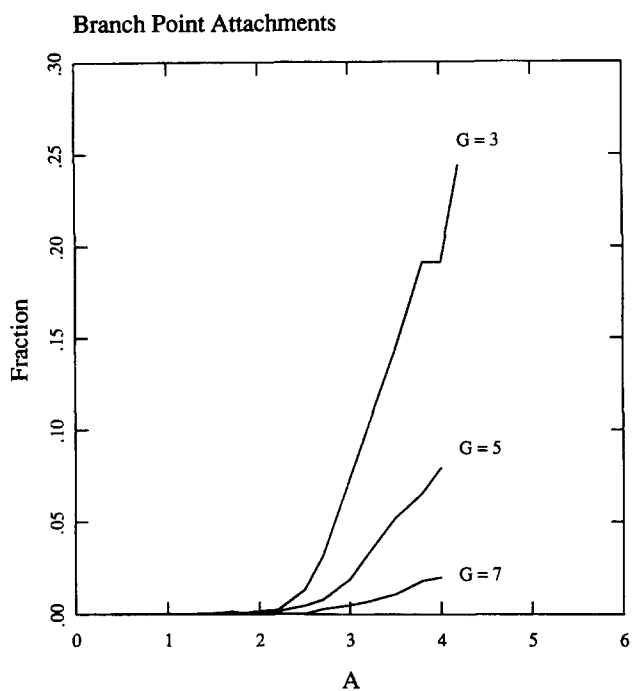


**Figure 10** The average fraction of branch points exactly three spacers away from the termini found interacting with the basal plane

to compensate for the loss of entropy, then the net interaction between the molecule and the barrier is repulsive<sup>9</sup>. The desorption region in *Figure 12* corresponds to those values of  $G$  and  $A$  for which the dendrimer desorbs rapidly from the surface over the time scale of the simulation.

At slightly larger  $A$  values we enter a region of weak adsorption. In this region, dendrimers generally stay in contact with the plane over the entire course of the simulation. However, the total number of contacts is

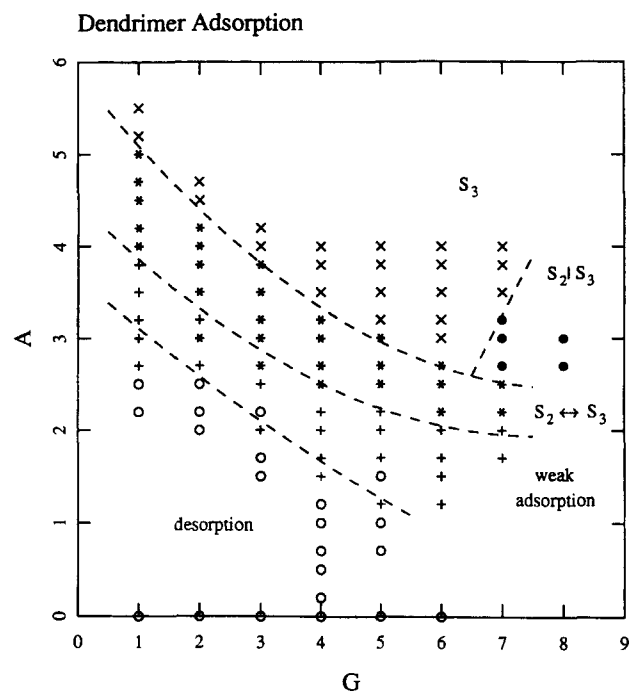


**Figure 12** Model dendrimers exhibit five classifications of behaviour, corresponding to the five regions shown on this diagram. This is not a true phase diagram, since there are no abrupt changes in behaviour from one region to the next

relatively small, and the global dimensions of the dendrimer, as measured by the various components of the radius of gyration, are not far from those of a desorbed dendrimer.

The boundary between these two regions drops with increasing  $G$  (as do most of the boundaries on the phase diagram). At large  $G$  the molecule possesses many sticky sites, and all of these must be removed simultaneously before the molecule can desorb.

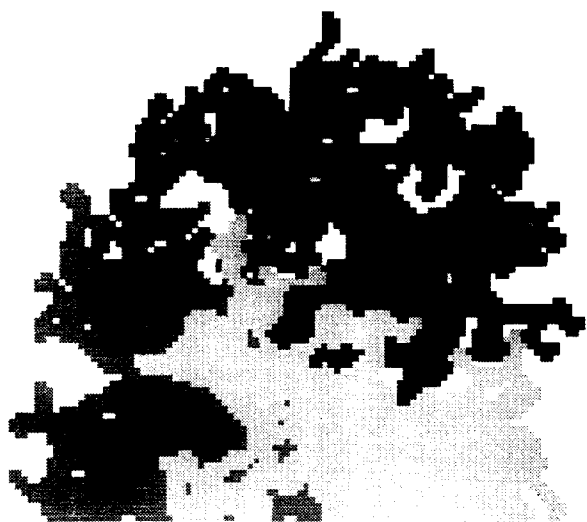


**Figure 13** Projection of a  $G = 7$  dendrimer in state  $S_2$ . Only two dendrons are in contact with the adsorption surface. This dendrimer was prepared at  $A = 3.2$

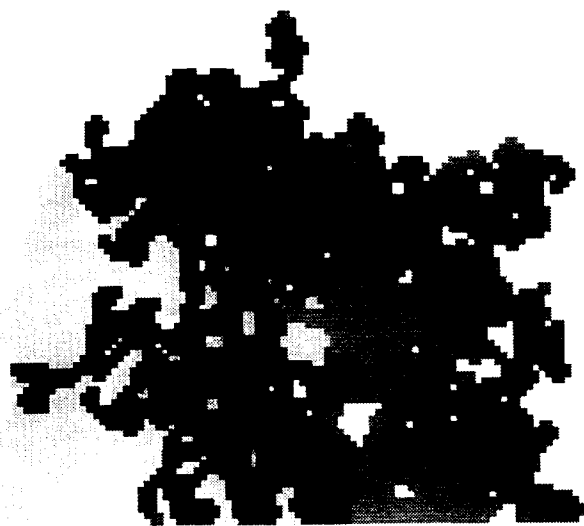


**Figure 14** Projection of a  $G = 7$  dendrimer in state  $S_3$ . All three dendrons are in contact with the adsorption surface. This dendrimer was prepared at  $A = 3.2$

At still larger  $A$  values, the dendrimer enters a region of interesting behaviour, denoted in *Figure 12* with the label  $S_2 \leftrightarrow S_3$ . Here the dendrimer tends to be found in either one of two states, denoted  $S_2$  or  $S_3$ . When in  $S_3$ , three dendrons are simultaneously in contact with the surface, while in  $S_2$ , only two of the three dendrons make contact, and the third sits 'up in the air', so to speak, as displayed in *Figures 13* and *14*. Furthermore, within this region of the phase diagram, and over the time scale of the simulation, relatively frequent transitions between the two states are observed. This implies that the two states have comparable free energies, at least within this particular region of the phase diagram. *Figure 15* displays the average energy difference between the two states, within this region of the phase diagram, as a function of  $G$ . In the higher generations,  $S_3$  is lower in energy by about 8 or 10  $kT$ . It follows that  $S_2$  is stabilized relative to  $S_3$  by having a larger entropy, and of course, it stands to reason that the system with one detached dendron would have both a larger energy and a larger

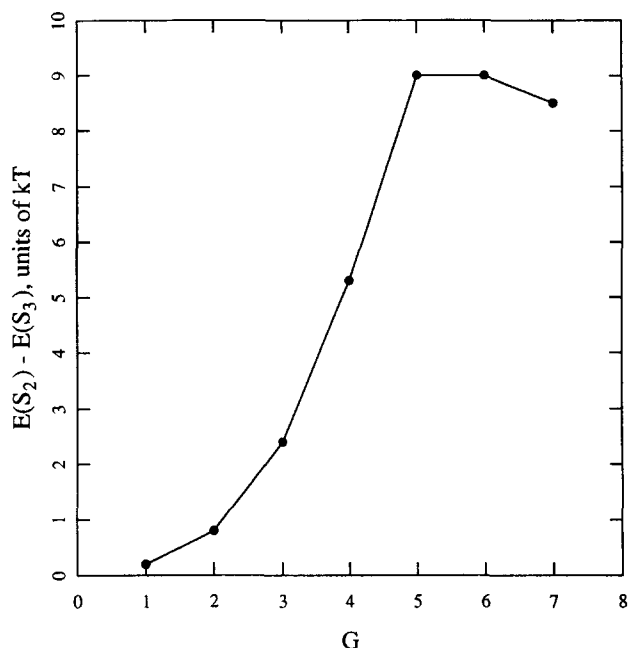


**Figure 15** Average energy difference between states  $S_2$  and  $S_3$  throughout the region denoted  $S_2 \leftrightarrow S_3$  in *Figure 12*, displayed as a function of  $G$

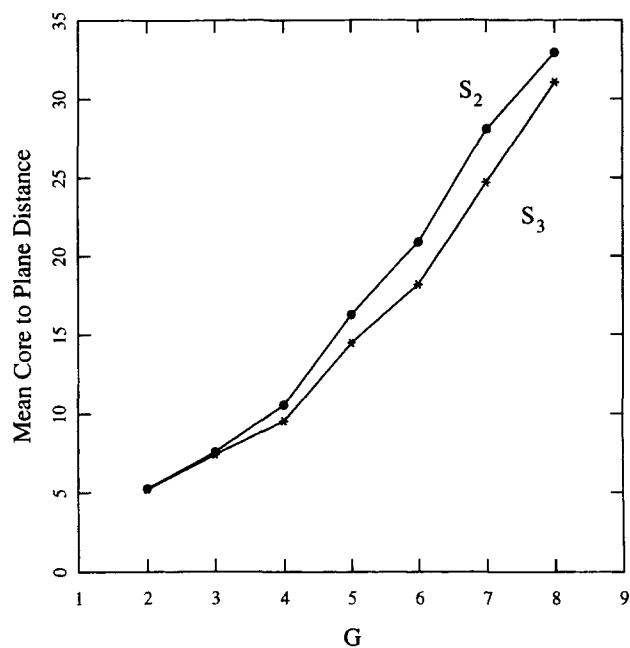


**Figure 16** Average core height throughout the region denoted  $S_2 \leftrightarrow S_3$  for dendrimers either in  $S_2$  or  $S_3$

entropy. *Figure 16* demonstrates that the core of the dendrimer lies approximately two or three length units higher in  $S_2$  than in  $S_3$ , in this region of the phase diagram and in the higher generations, which also stands to reason.

At still higher  $A$  values, we enter a region labelled  $S_3$ . Here the dendrimer is found almost exclusively (>99% of the time) in state  $S_3$ . If initiated in  $S_3$ , the dendrimer typically remains in  $S_3$ , and if initiated in  $S_2$ , it eventually transforms into  $S_3$  and stays there. Therefore, the free energy of  $S_3$  is sufficiently lower than that of  $S_2$  that the equilibrium strongly favours  $S_3$ .

We have been unable to estimate the free energy barrier between  $S_2$  and  $S_3$ , but it is reasonable to expect that this barrier increases with  $G$ . Presumably, to undergo the transition  $S_2 \rightarrow S_3$ , segments from the unadsorbed dendron must reach down and make contact with the plane. If the adsorbed dendrons are very large, they prevent this from happening. Therefore, we expect a region of the phase diagram in which  $S_3$  is considerably more stable than  $S_2$ , but in which the dendrimer becomes effectively trapped in  $S_2$  because the free energy barrier into  $S_3$  is too large. This behaviour is found in the region labelled  $S_2|S_3$ . In this region, the dendrimer is observed to remain in the state,  $S_2$  or  $S_3$ , in which it was initiated.

## CONCLUSIONS

The parallel and perpendicular components of the radius of gyration and the average distance between the core and the adsorption plane change with increasing adsorption strength in ways consistent with the molecule flattening down and spreading out on the surface. Surprisingly, the overall radius of gyration changes much less noticeably, this is due to mutual compensation between the changes in the parallel and perpendicular components.

At small  $G$  and large  $A$ , most sticky segments can make contact with the plane because the molecule is highly deformable. At large  $G$ , a smaller fraction of the segments are able to make contact, even for  $A$  very large, because the dendrimer is much less deformable. In any case, the sticky segments at or near the termini of the molecule are more likely to be in contact than those nearer the core.

Desorption is observed at small  $A$ , as expected. The value of  $A$  needed to maintain adsorption decreases with increasing  $G$ .

At sufficiently large  $A$  the dendrimer prefers one of two states,  $S_2$  or  $S_3$ , in which either two or three dendrons, respectively, make contact with the surface plane. Of the two,  $S_2$ , has both higher energy and entropy; the unattached dendron is free to explore more conformations but has no energy of adsorption. Because of this interplay of energy and entropy, there are values of  $A$  and  $G$  for which the two states have comparable free energies and, therefore, frequent transitions between the two states are observed. Then there are values of  $A$  and  $G$  for which  $S_3$  is more stable than  $S_2$  and for which transitions only in the direction  $S_2 \rightarrow S_3$  are observed. Finally, there are values of  $A$  and  $G$  for which the free energy barrier between  $S_2$  and  $S_3$  is so large that transitions in either direction are not observed.

## REFERENCES

- 1 deGennes, P. G. and Hervet, H. *J. Phys.* 1983, **44**, L351
- 2 Naylor, A. M., Goddard III, W. A., Kiefer, G. E. and Tomalia, D. A. *J. Am. Chem. Soc.* 1989, **111**, 2339
- 3 Lescanec, R. L. and Muthukumar, M. *Macromolecules* 1990, **23**, 2280
- 4 Mansfield, M. L. and Klushin, L. I. *J. Phys. Chem.* 1992, **96**, 3994
- 5 Mansfield, M. L. and Klushin, L. I. *Macromolecules* 1993, **26**, 4262
- 6 Mansfield, M. L. *Polymer* 1994, **35**, 1827
- 7 Murat, M. and Grest, G. S. *Macromolecules* 1996, **29**, 1278
- 8 Tomalia, D. A. and Dvornic, P. R. *Nature* 1994, **372**, 617 (and references cited therein)
- 9 deGennes, P. G. 'Scaling Concepts in Polymer Physics'. Cornell University Press, Ithaca, 1979